Confirming the Unusual Temperature Dependence of the Electric-Field Gradient in Zn

Heinz Haas [1,2,*], Dmitry Zyabkin [3], Juliana Schell [2,4], Thien T. Dang [4], Ian C. J. Yap [5], Ilaria Michelon [6], Daniel Gaertner [7], Adeleh Mokhles Gerami [8], Cornelia Noll [9] and Reinhard Beck [9]

[1] Department of Physics and CICECO, University of Aveiro, 3810-193 Aveiro, Portugal
[2] EP Division, CERN, 1211 Geneve, Switzerland; juliana.schell@cern.ch
[3] Chair Materials for Electrical Engineering and Electronics, Institute of Materials Science and Engineering, Institute of Micro and Nanotechnologies MacroNano®, TU Ilmenau, Gustav-Kirchhoff-Strasse 5, 98693 Ilmenau, Germany; dmitry.zyabkin@cern.ch
[4] Institute for Materials Science and Center for Nanointegration Duisburg-Essen (CENIDE), University of Duisburg-Essen, 45141 Essen, Germany; thien.dang@uni-due.de
[5] Physikalisches Institut, Georg-August Universität Göttingen, 37077 Göttingen, Germany; iany0003@e.ntu.edu.sg
[6] Department of Physics and Astronomy, University of Padova, 35122 Padova, Italy; ilaria.michelon@cern.ch
[7] Institute of Materials Physics, University of Münster, 48149 Münster, Germany; daniel.gaertner@uni-muenster.de
[8] School of Particles and Accelerators, Institute for Research in Fundamental Sciences (IPM), Tehran P.O. Box 19395-5531, Iran; adeleh.mokhles.gerami@cern.ch
[9] Helmholtz-Institut für Strahlen- und Kernphysik, University of Bonn, 53115 Bonn, Germany; noll@hiskp.uni-bonn.de (C.N.); beck@hiskp.uni-bonn.de (R.B.)
* Correspondence: heinz.haas@cern.ch

Abstract: The electric-field gradient (EFG) at nuclei in solids is a sensitive probe of the charge distribution. Experimental data, which previously only existed in insulators, have been available for metals with the development of nuclear measuring techniques since about 1970. An early, systematic investigation of the temperature dependence of the EFG in metals, originally based on results for Cd, but then also extended to various other systems, has suggested a proportionality to $T^{3/2}$. However, later measurements in the structurally and electronically similar material Zn, which demonstrated much more complex behavior, were largely ignored at the time. The present experimental effort has confirmed the reliability of this unexpected behavior, which was previously unexplained.

Keywords: nuclear quadrupole interaction; electric field gradients; Zn metal; temperature dependence; PAC measurements

1. Introduction

The study of the interaction of nuclear quadrupole moments (Q) with the charges of the surrounding can give detailed insight into the electronic distribution that creates bonding in solids. Since the discovery of nuclear quadrupole resonance (NQR) in the middle of the last century [1], as well as the qualitative understanding of the temperature effects involved [2], an abundant number of experimental and theoretical studies of molecular and ionic solids have been performed. Electric field gradients (EFG), the second derivative of the charge density V_{zz} at the nuclear site, which determine the quadrupole interaction constant $\nu_Q = eQV_{zz}/h$, were thus understood quite early for such materials in a semiquantitative manner.

For metallic solids, on the other hand, the applications of a radiofrequency technique like NQR are severely limited, and therefore, only very few systems could be investigated earlier. With the introduction of perturbed angular correlation (PAC) [3] and perturbed angular distribution (PAD) [4] spectroscopy in the early 1970s, these limitations disappeared. In addition, such nuclear methods also allow the study of impurities, even at extreme

dilutions. Thus, since about 50 years ago, an abundant amount of experimental information on nuclear quadrupole interactions in metals has quickly evolved. It has become evident, however, that the electronic structure theory techniques available at the time were not appropriate for a quantitative calculation of the EFG—even in simple sp-metals. Thus, for the interpretation of the experimental results, including those regarding EFG temperature dependence, recourse to semiquantitative approximations had to be accepted.

A large-scale, systematic study of the EFG (here for simplicity called *q*) temperature dependence [5], however, generated a uniform description of a suggested "law" as *{q(T)-q(0)}/q(0)*, very closely proportional to $T^{3/2}$. This dependence apparently had so much appeal that it was later used in practically all cases, thus implying that lattice vibrations were the only effective sources. Other early attempts to account for EFG temperature dependence have tried to incorporate the structural and vibration changes [6,7] in their approaches. These calculations, using screened pseudopotentials, however, could at best only qualitatively account for the experimental data as quantitative electronic structure calculation for EFG was not possible at the time.

The situation changed dramatically with the availability of reliable density functional calculations for metals [8,9]. Such techniques were actually used in two recent theoretical attempts to account for EFG in Cd and Zn as function of temperature [10,11]. These calculations, however, largely concentrated on the effect of lattice vibrations, which were apparently stimulated by the $T^{3/2}$ "law". Unfortunately, these works, as well as all previous discussions, ignored the fact that experimental data for EFG temperature dependence in Zn, which contradicted the proposed universal law, have been available for quite some time via Mössbauer spectroscopy [12], nuclear magnetic resonance [13] and, in particular, perturbed angular correlation measurements [14,15]. Figure 1 demonstrates the dramatic failure of the $T^{3/2}$ law in accounting for the PAC results for ^{111}Cd (5/2$^+$) in Zn. The present investigation was initiated with the purpose of testing the correctness of these early PAC measurements and to add new data points. That seems especially important as such data have been the basis for a recent quantitative explanation of the EFG temperature dependence of Zn and Cd [16].
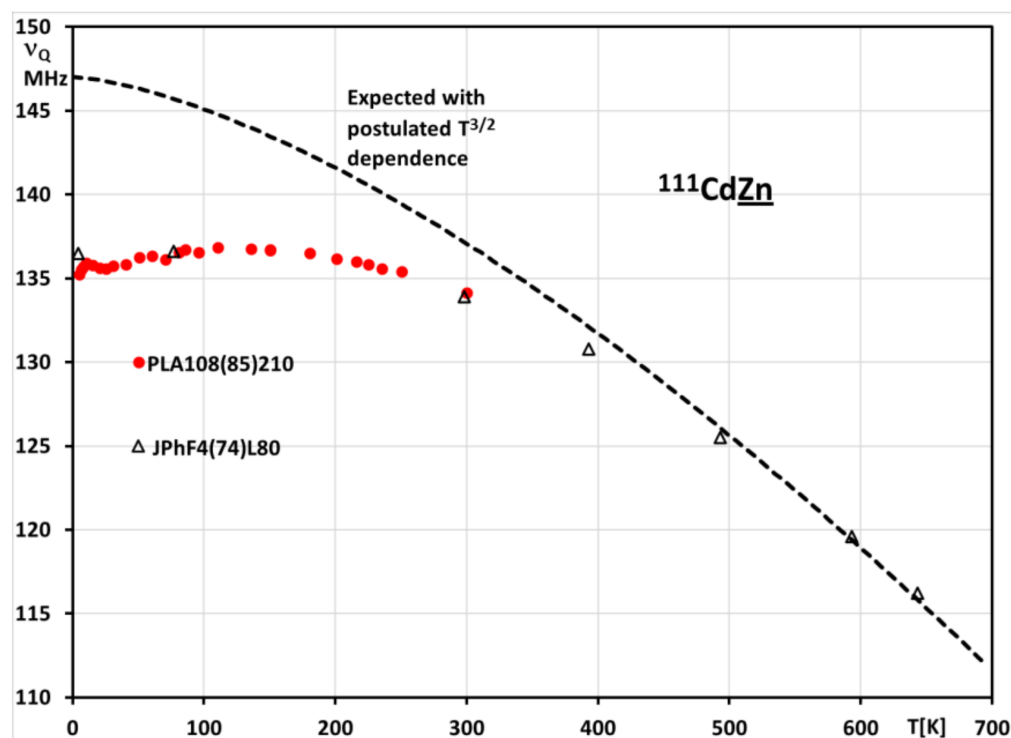

Figure 1. Existing data for ν_Q for ^{111}Cd in Zn as a function of temperature confronted by expected dependence from $T^{3/2}$ "law". References: JPhF4(74)L80 [14], PLA108(85)210 [15].

2. Materials and Methods

In the present measurements, two different samples were employed. For the initial experiment series up to 540 K, a commercially obtained single crystal of Zn, with a thickness of 0.5 mm and dimensions of 4 by 5 mm (MaTecK GmbH, Jülich, Germany), was surface-cleaned, first by polishing and then by sputtering with an Ar beam. For the later measurements (closer to the Zn melting point of 419.5 °C (592.7 K)), a 0.1 mm thick, rolled foil (Goodfellow Cambridge Limited, Huntingdon, England) was scratched using a scalpel immediately prior to implantation so as to create a clean surface.

For the initial PAC experiments, the necessary ^{111}In activity was commercially obtained and implanted at room temperature with an energy of 80 keV and an incidence angle of 10° (from the surface normal) at the Bonn Radioisotope Separator and Implanter (BONIS) facility in Bonn, Germany [17,18]. Monte Carlo simulations, using SRIM (Stopping and range of ions in matter) software with TRIM (Transport of ions in matter) [19], provided an average implantation depth of the order of 30 nm. The latter-used foil sample was doped with ^{111}In at a 30 keV implantation energy produced by the high-energy proton irradiation of uranium-carbide at the ISOLDE-CERN [20] online isotope separator.

Before the measurements, an annealing in the Ar atmosphere at 473 K was performed on both samples, as the originally implanted, single crystal showed, in agreement with [14], only a distribution of EFG values, presumably due to the lattice defects created by the implantation process.

PAC measurements were carried out at the ISOLDE-CERN [21] solid-state facilities, with the initial single-crystal runs employing an analogue 4-detector system with an angle of 90° between the detectors and BaF$_2$ scintillator crystals coupled to photomultiplier tubes [22]. The hardware selected signals using the photopeaks of the start and stop γ-rays in the cascade in [111]Cd following the EC decay of [111]In. Their time-differences were used to record the 12 (4 for 180° spectra and 8 for 90° spectra) possible coincidence time-spectra using the DOS-based software UNCPAC [23]. For data acquisition and storage, the Ortec Model 918 ADCAM Multichannel Buffer (MCB) was used and controlled via a dedicated dual-port memory interface on a computer. In all measurements, the surface normal of the single crystal, the crystal c-axis, was oriented in the detector plane at 45° between the detectors as well as was possible.

The measurements with the polycrystalline foil sample, concentrating in the higher temperature region, were made using the KATAME digital spectrometer [24], with an array of 6 lanthanum–bromide scintillation detectors.

For the experiments carried out below room temperature, the sample, contained in a glass tube under N$_2$ gas, was measured in a Dewar filled with liquid nitrogen or an acetone-solid CO$_2$ slush. Higher temperatures were obtained in an insulated glass tube heated with resistive wire under slight gas flow, controlled by a thermocouple.

For the 12, respectively 30, time-spectra recorded the normalized and background-corrected $W(\theta,t)$. The conventional ratio function given by Equation (1) was fitted to the corresponding theoretical perturbation function, appropriate to the crystal orientation, to obtain the quadrupole interaction frequencies ν_Q.

$$R(t) = 2\frac{W(180°,t) - W(90°,t)}{W(180°,t) + 2W(90°,t)} \tag{1}$$

3. Results

Selected PAC spectra are shown in Figure 2a,b. The results for the effective nuclear quadrupole coupling constant obtained at the various temperatures are summarized in Table 1.
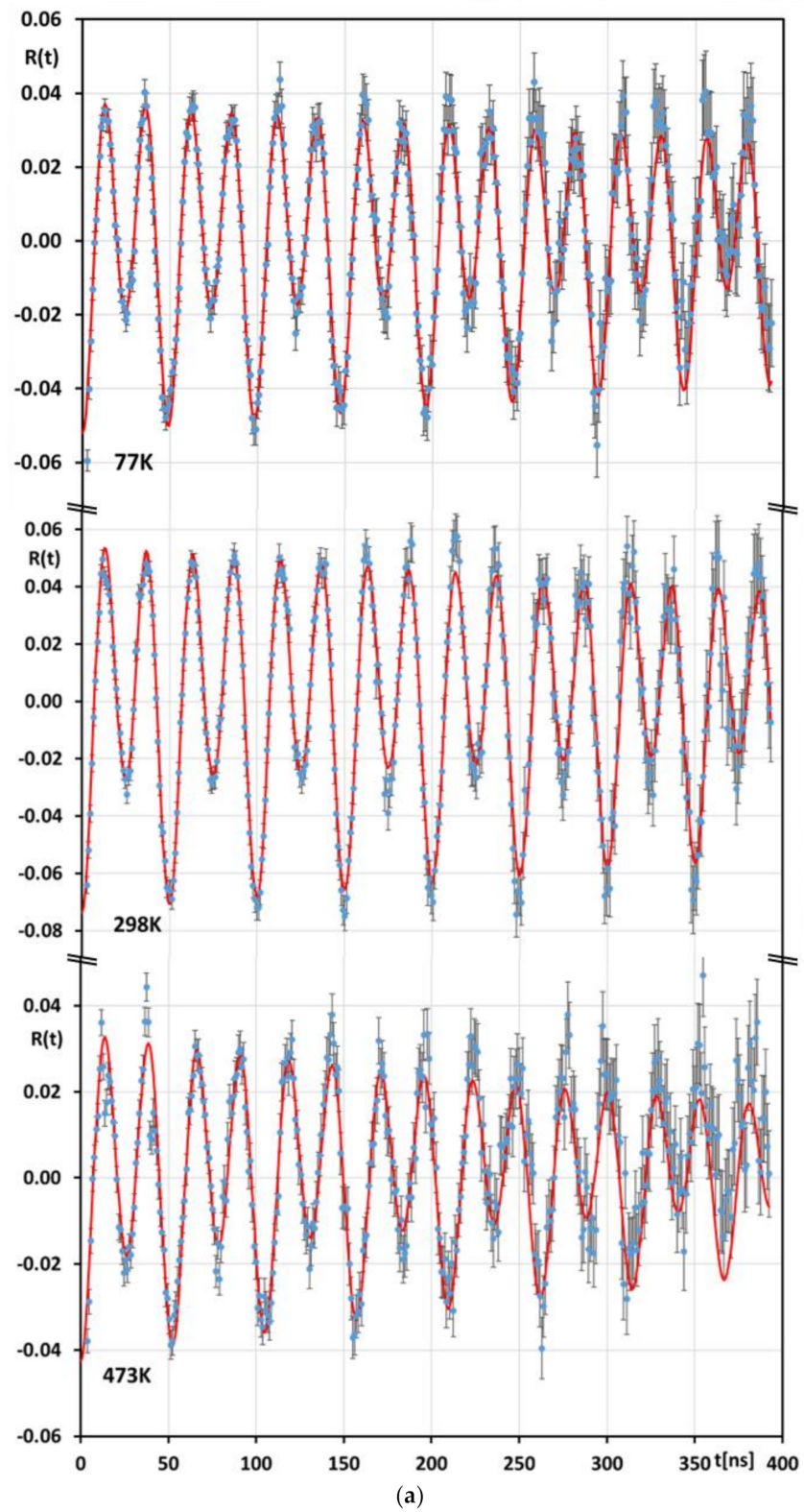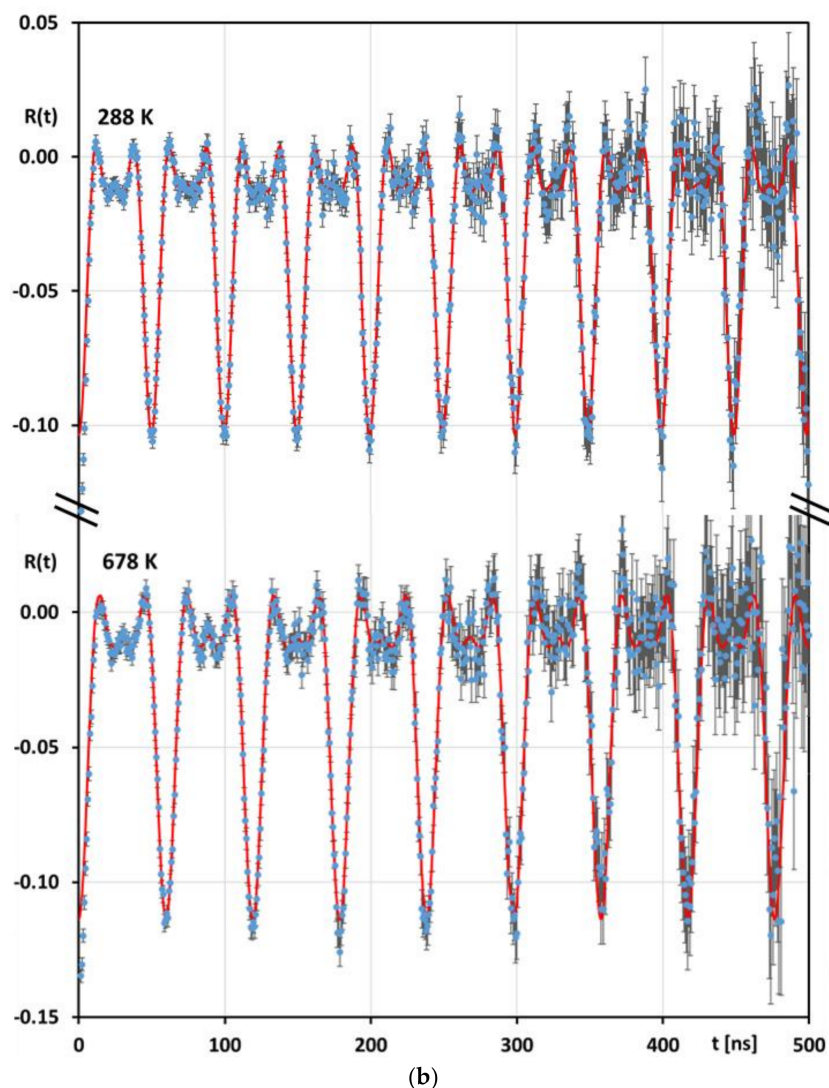
(**a**)

Figure 2. *Cont.*

(b)

Figure 2. (**a**) Examples for observed PAC spectra taken with the single-crystal sample. The red, solid curves show the least-squares fits that give the quadrupole interaction parameters presented in Table 1. The clear difference between the EFGs is visualized by comparing the spectra obtained at 77 K or 298 K with the spectrum taken at 473 K, and analogous in Figure 2b. (**b**) Examples for observed PAC spectra taken with the polycrystalline sample. The pattern seen is characteristic of a random EFG orientation.

Table 1. Nuclear quadrupole coupling constant ν_Q measured for ^{111}Cd ($5/2^+$) in a Zn single crystal as function of temperature. The lower four rows present data from the experiments with polycrystalline Zn.

Temperature [K]	ν_Q [MHz]	Err [MHz]
77	135.92	0.20
203	135.68	0.20
298	133.31	0.15
343	132.43	0.20
423	129.11	0.25
473	127.23	0.25
543	123.72	0.30
288	133.69	0.10
603	118.58	0.10
653	114.32	0.10
678	111.94	0.10

Please note that the tubular furnace used for high-temperature measurements has an uncertainty of ± 5–$10\ ^\circ$C.

4. Discussion

Measurements with the earlier, standard PAC technique, including our single-crystal data, must be adjusted according to the uncertainty of the time-calibration. Correcting for the at-most 0.3 MHz different frequencies at 77 K of the various experiments, our results agree very well with the earlier data in the low-temperature range of [15] and also with the datapoint at room temperature reported by [14]. Our second series of measurements, using digital frequency measurement and improved temperature control, was triggered by the fact that the frequencies at 473 K and 543 K appeared to deviate from the data in [14] by more than the combined temperature and frequency uncertainty. In addition, in their pioneering study of EFG temperature dependence for Cd in Cd [25], the authors of reference [14] made a serious temperature error, later corrected in [4]. Our new, precise data, however, fully agree with their results for Cd in Zn.

All frequencies, properly corrected, are presented in Figure 3 relative to the ν_Q determined as 135.32(10) MHz for T = 0. This result is considerably smaller than the frequency of 136.5(14) MHz at 4.2 K reported in [14], although it is still within the (very liberally) quoted error. It evidently agrees with the results of [15] of around 4.2 K, taking as error 0.3 MHz. A new, precise measurement at 4.2 K could, however, be extremely worthwhile as, in [15], the data around 4 K appear to show a yet-inexplicable scatter.
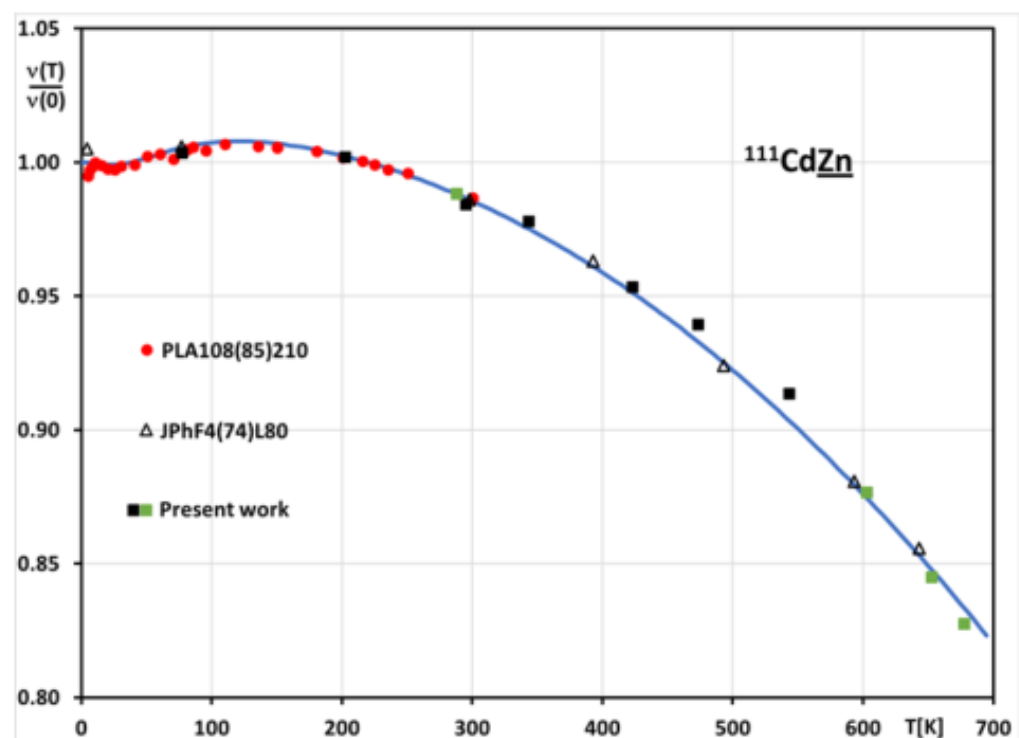

Figure 3. Normalized temperature dependence of EFG for Cd in Zn, including the present data; the green squares denote the results using the polycrystalline sample. The blue curve shows the one-parameter fit described in the text. References: JPhF4(74)L80 [14], PLA108(85)210 [15].

The now well-confirmed trend is in good agreement with the recently proposed functional temperature dependence for EFG [16], making use of reanalyzed structural data for the calculation of EFG for the static lattice with the now-standard density functional technique. For determining the vibrational dependence of EFG, the proportionality with the average Debye–Waller factor as function of temperature, as obtained via a new analysis of experimental vibrational data, was employed, multiplied by one fitted parameter.

Figure 3 demonstrates reasonably well the extent to which this treatment can explain all of the now-available experimental data. Obviously, the quite minor discrepancies still existing could warrant a series of considerably more precise PAC measurements using the time precision that is now possible with fully digital electronics. This project will, of course, also require temperature control that is much more precise than the one used to date. Only with these precision data could the actual functional dependence through the vibrational motion be checked in detail. The reliability of the final accuracy obtainable in this way would, unfortunately, still be limited by the dependence on the precision of the experimental thermal displacement amplitudes presently obtainable from X-ray analysis, with Zn actually being the non-cubic metal from which the best such data are available.

5. Conclusions

The present study used the PAC spectroscopy method to probe the temperature dependence of the nuclear quadrupole coupling constant ν_Q in Zn crystals implanted with the nuclear probe ^{111}In(^{111}Cd). Our results agree well with previous data [14,15] and demonstrate the complex temperature dependence of the electric field gradient, which is extremely different from that which was previously expected due to the $T^{3/2}$ law. The fact that the corresponding data for ν_Q in Cd ([4,5,25] and others) quite closely follow this simple tendency must thus be fortuitous.

References and Note

1. Dehmelt, H.G.; Krueger, H. Quadrupol-Resonanzfrequenzen von Cl- und Br-Kernen in kristallinem Dichloraethylen und Methylbromid. *Z. Phys.* **1951**, *129*, 401–415. [CrossRef]
2. Bayer, H. Zur Theorie der Spin-Gitterrelaxation in Molekülkristallen. *Z. Phys.* **1951**, *130*, 227–238. [CrossRef]
3. Raghavan, P.; Raghavan, R.S. Nuclear quadrupole interaction in cadmium metal. *Phys. Rev. Lett.* **1971**, *27*, 724. [CrossRef]
4. Bleck, J.; Butt, R.; Haas, H.; Ribbe, W.; Zeitz, W. In-beam measurements of the nuclear quadrupole interaction in cadmium metal. *Phys. Rev. Lett.* **1972**, *29*, 1371. [CrossRef]
5. Christiansen, J.; Heubes, P.; Keitel, R.; Klinger, W.; Loeffler, W.; Sandner, W.; Witthuhn, W. Temperature dependence of the electric field gradient in noncubic metals. *Z. Phys. B Cond. Matt.* **1976**, *24*, 177–187. [CrossRef]
6. Nishiyama, K.; Dimmling, F.; Kornrumpf, T.; Riegel, D. Theory of the temperature dependence of the electric field gradient in noncubic metals. *Phys. Rev. Lett.* **1976**, *37*, 357. [CrossRef]
7. Nishiyama, K.; Riegel, D. Recent developments in the analysis of electric field gradients in metals. *Hyperfine Interact.* **1978**, *4*, 490–508. [CrossRef]
8. Blaha, P.; Schwarz, K.; Dederichs, P.H. First-principles calculation of the electric-field gradient in hcp metals. *Phys. Rev. B* **1988**, *37*, 2792. [CrossRef]
9. Blaha, P.; Dufek, P.; Schwarz, K.; Haas, H. Calculation of electric hyperfine interaction parameters in solids. *Hyperfine Interact.* **1996**, *97*, 1–10. [CrossRef]

10.　Torumba, D.; Parlinski, K.; Rots, M.; Cottenier, S. Temperature dependence of the electric-field gradient in hcp-Cd from first principles. *Phys. Rev. B* **2006**, *74*, 144304. [CrossRef]

11.　Nikolaev, A.V.; Chtchelkatchev, N.M.; Salamatin, D.A.; Tsvyashchenko, A.V. Towards an ab initio theory for the temperature dependence of electric field gradients in solids: Application to hexagonal lattices of Zn and Cd. *Phys. Rev. B* **2020**, *101*, 064310. [CrossRef]

12.　Potzel, W.; Adlassnig, W.; Närger, U.; Obenhuber, T.; Riski, K.; Kalvius, G.M. Temperature dependence of hyperfine interactions and anisotropy of recoil-free fraction: A Mössbauer study of the 93.3 keV resonance of ^{67}Zn in single crystals of zinc metal. *Phys. Rev. B* **1984**, *30*, 4980. [CrossRef]

13.　Bastow, T.J. ^{67}Zn NMR in zinc metal. *J. Phys. Condens. Matter.* **1996**, *8*, 11309. [CrossRef]

14.　Raghavan, P.; Raghavan, R.S.; Kaufmann, E.N.; Krien, K.; Naumann, R.A. Nuclear quadrupole interaction of ^{111}Cd in zinc (by PAC). *J. Phys. F Met. Phys.* **1974**, *4*, L80. [CrossRef]

15.　Hermans, L.; van Cauteren, J.; Rots, M. Anomalous low temperature behaviour of the electric field gradient at ^{111}Cd in cadmium and zinc. *Phys. Lett. A* **1985**, *108*, 210–214. [CrossRef]

16.　Haas, H. Temperature Dependence of Electric-Field Gradient in Zn and Cd: Ending the $T^{3/2}$ "Myth". Manuscript to Be Submitted to Physical Review B. Available online: https://indico.cern.ch/event/1182057/ (accessed on 3 July 2022).

17.　Freitag, K. A facility for ion implantation in samples colder than 0.5 K. *Radiat. Eff.* **1979**, *44*, 185. [CrossRef]

18.　Schell, J.; Lupascu, D.C.; Carbonari, A.W.; Mansano, R.D.; Junior, I.S.R.; Dang, T.T.; Anusca, I.; Trivedi, H.; Johnston, K.; Vianden, R. Ion implantation in titanium dioxide thin films studied by perturbed angular correlations. *J. Appl. Phys.* **2017**, *121*, 145302. [CrossRef]

19.　Ziegler, J.F.; Ziegler, M.D.; Biersack, J. SRIM—The Stopping and Range of Ions. *Matter. Nucl. Instr. Meth.* **2010**, *B268*, 1818–1823. [CrossRef]

20.　Catherall, R.; Andreazza, W.; Breitenfeldt, M.; Dorsival, A.; Focker, G.J.; Gharsa, T.P.; Giles, T.J.; Grenard, J.-L.; Locci, F.; Martins, P.; et al. The ISOLDE facility. *J. Phys. G Nucl. Part. Phys.* **2017**, *44*, 094002. [CrossRef]

21.　Johnston, K.; Schell, J.; Correia, J.G.; Deicher, M.; Gunnlaugsson, H.P.; Fenta, A.S.; David-Bosne, E.; Costa, A.R.G.; Lupascu, D.C. The solid state physics programme at ISOLDE: Recent developments and perspectives. *J. Phys. G Nucl. Part. Phys.* **2017**, *44*, 104001. [CrossRef]

22.　Schell, J.; Schaaf, P.; Lupascu, D.C. Perturbed angular correlations at ISOLDE: A 40 years young technique. *AIP Adv.* **2017**, *7*, 105017. [CrossRef]

23.　Hofsaess, H.; Deicher, M. Perturbed γ-γ-Angular Correlation Program. Version 5.25 of 20-jan-2002. The UNCPAC software has been mostly developed by H. Hofsäss based on a first version called PAC written by H. Hofsäss and M. Deicher in 1988.

24.　Nagl, M.; Vetter, U.; Uhrmacher, M.; Hofsäss, H. A new all-digital time differential γ-γ angular correlation spectrometer. *Rev. Sci. Instrum.* **2010**, *81*, 073501. [CrossRef]

25.　Raghavan, R.S.; Raghavan, P. Anomalous temperature dependence of the quadrupole interaction in cadmium. *Phys. Lett. A* **1971**, *36*, 313. [CrossRef]